COMPARING MODIS AND ETM$^+$ IMAGE DATA FOR INLAND WATER STUDIES: SPATIAL RESOLUTION CONSTRAINTS

Comparação de Imagens MODIS e ETM para Estudo de Águas Interiores: Imposições da Resolução Espacial

Evlyn Márcia Leão de Moraes Novo [1]
Claudio Clemente Faria Barbosa[1]
John M.Melack [2]
Ramon Moraes de Freitas[1]
Fernanda Titonelli[1]
Yosio Shimabukuro[1]

[1] Instituto Nacional de Pesquisas Espaciais – INPE
Coordenação de Observação da Terra
12 201970 – São José dos Campos – SP, CP. 515
evlyn@ltid.inpe.br

[2] University of California, Santa Barbara, USA
Bren School of Environmental Science and Management,
Santa Barbara, CA 93106, USA,
melack@lifesci.lscf.ucsb.edu

RESUMO

O objetivo desse artigo é apresentar os resultados de um estudo voltado à comparação do desempenho das imagens MODIS de resolução moderada (250 m e 500 m) com o de imagens com maior resolução espacial como as imagens do sensor ETM$^+$ no tocante a sua capacidade para o mapeamento de feições relevantes para o estudo dos sistemas aquáticos. Para realizar essa comparação, foram obtidas simultaneamente imagens ETM+ e MODIS sobre a região da planície do Lago Grande de Curuai. Para que se tornassem comparáveis, ambos os conjuntos de imagens foram georreferenciados e reamostrados para um tamanho de pixel de 100 m x 100m com o auxílio do interpolador pelo vizinho mais próximo de modo a compatibilizar o tamanho da grade sobre a qual se aplicariam os processamentos subseqüentes. Esse procedimento foi adotado com base na suposição de que a resolução efetiva dos sensores seria pouco afetada devido ao maior poder de resolução radiométrica dos dados MODIS. Após a organização da base de dados, as imagens foram submetidas a testes visando identificar o melhor procedimento para gerar um mapa com a distribuição de ilhas, rios e canais da região de estudo. Os testes indicaram que a melhor abordagem foi a de segmentação e classificação não supervisionada da fração sombra derivada da aplicação do modelo linear de mistura as imagens ETM+ e MODIS. Os mapas resultantes da segmentação e classificação foram transformados em vetores e gerados polígonos representativos das feições classificadas genericamente em lagos (água) e ilhas (terra). Procedeu-se então a análise da distribuição dos polígonos em termos da freqüência de tamanho de ilhas e lagos mapeáveis. Os resultados permitiram verificar que em termos de área total mapeada pelos sensores ETM+ e MODIS, as diferenças chegam a 11 %. Entretanto, a análise da distribuição de polígonos mapeados indica que há um grande número de polígonos detectados pelas imagens MODIS que não puderam ser recuperados pela imagem ETM+. Esses resultados sugerem que as melhorias apresentadas pelo sensor MODIS no tocante à resolução espectral e radiométrica podem compensar em algumas situações específicas a degradação da resolução espacial. Na realidade, os resultados mostram que nas condições em que foi realizado este experimento as imagens MODIS podem ter um desempenho melhor do que o de imagens do sensor ETM+ reamostradas para 100m x 100m. Isto explicaria a pequena diferença de desempenho no tocante ao computo final da área ocupada por superfícies líquidas.

Palavras chaves: Imagens MODIS, Imagens ETM$^+$, Sistemas Aquáticos, Resolução Espacial.

ABSTRACT

The objective of this paper is to compare the performance of medium spatial resolution (250 m and 500 m) Terra MODIS images to finer resolution Landsat ETM+ images. MODIS Terra images have high frequency of acquisition (1 day revisit at high latitudes) and that makes them more useful for inland water studies. Assessing the performance of ETM and MODIS to map relevant features for the functioning of aquatic systems is very important for fostering water resource remote sensing. To carry out the comparison, concurrent ETM^+ and MODIS images were acquired over the Lago Grande de Curaui Lake. The images were georeferenced and resample to the 100 x 100 m ground resolution using a next neighbor algorithm to make the data comparable. The resampling rationale was making the digital processing easier, without changing the effective resolution properties of the original data. It was assumed that the improved MODIS radiometric resolution as compared to the ETM^+ would make both data set comparable at a 100m x 100m resolution. In the next step, a series of tests were carry out in order to define the best approach to map aquatic system features such as lakes, islands, and levees in the study area. The tests indicated that the best approach was the segmentation of the shadow fraction derived from the application of the linear unmixing model to both ETM+ and MODIS images. The segmentation was then followed by the application of a non-supervised region classifier. The final classes were mapped into two categories: lakes (water) and island (land). The polygon distribution generated by the classification procedure was then statistically analyzed to assess the polygon size frequency of features mapped by each data set. The results showed that ETM+ and MODIS were able to recover the water surface area in the studied region with a difference of 11 %. The analyses of polygon distribution, however, showed that there were many polygons which were detected in MODIS image data, but not in ETM+ image data. This result suggests that the spectral and radiometric resolution improvements presented by MODIS image tend to compensate for the losses in spatial resolution. That is to say that under the boundary conditions adopted in this study, MODIS images performed better than degraded ETM^+ images of 100m x 100m. This explains the small difference in performance presented by comparing two sensors with such large differences in nominal spatial resolution.

Keywords: MODIS Images, EMT^+ images, Aquatic Systems, Spatial Resolution.

1. INTRODUCTION

This paper reports an experiment performed to assess the suitability of MODIS spatial resolution for studying Amazon aquatic systems compared to that of Landsat/ETM^+ images degraded to 100 m x 100 m. The assumption is that the spatial resolution will not be a major constraint for the retrieval of ground information because it is compensated by the improved radiometric and spectral resolution.

The remote sensing of inland waters was always behind of Ocean, Atmospheric and Land applications because the sensors available did not meet the requirements needed to cope with a target that displays a huge variability in space and time. The water color sensors developed for ocean applications (Kampel and Novo, 2005) have poor spatial resolution and the radiometric resolution is not tuned to deal with scenes undergoing sharp changes in the reflected signal. Land sensors such as the Thematic Mapper on board of Landsat satellite series do not have the radiometric sensitivity to account for subtle changes in water reflectance (Kirk, 1994).

MODIS is the principal high temporal frequency global mapping sensor on-board NASA's Earth Observation System (EOS) (http://modarch.gsfc.nasa.gov/MODIS/), Terra (February 2000 - present) and Aqua, (June 2002 - present) satellites. Terra and Aqua are at near-polar, Sun-synchronous orbits, and are crossing the Equator three hours apart: Terra at 10:30AM, descending, while Aqua at 1:30PM, ascending. Thus, near global coverage is achieved by MODIS in a single day, at spatial resolutions spanning from 250 m to 1000 m according to various application requirements. These features suggest that MODIS data might be useful for studying large inland aquatic systems such as those comprised by the Amazon River Basin.

MODIS is an optical scanner that measures Earth radiance in 36 bands, ranging from 0.4 to 14 μm and presents substantial improvements in bandwidths and radiometric resolution which are fundamental for inland water studies. In addition to these new features, continuous global data sets and corresponding science products with improved quality have been produced with constant on-orbit calibration. Table 1 summarizes the main MODIS features. Table 2 summarizes the information derived from MODIS products designed for both land and ocean applications.

TABLE 1 – MODIS SPECIFICATIONS
(http://modis.gsfc.nasa.gov/about/specs.html)
[1] Bands 1 to 19 are in nm; Bands 20 to 36 are in µm; Quantization= 12 bits; Spatial Resolution: 250m (bands 1,2); 500m (bands 3-7); 1000 m (8-36)

Primary Use [1]	**Band**	**Bandwidth**
Land/Cloud/Aerosols Boundaries	1	620 – 670
	2	841 – 876
Land/Cloud/Aerosols Properties	3	459 – 479
	4	545 – 565
	5	1230 – 1250
	6	1628 – 1652
	7	2105 – 2155
Ocean Color/ Phytoplankton/ Biogeochemistry	8	405 – 420
	9	438 – 448
	10	483 – 493
	11	526 – 536
	12	546 – 556
	13	662 – 672
	14	673 – 683
	15	743 – 753
	16	862 – 877
Atmospheric Water Vapor	17	890 – 920
	18	931 – 941
	19	915 – 965
Surface/Cloud Temperature	20	3.660 - 3.840
	21	3.929 - 3.989
	22	3.929 - 3.989
	23	4.020 - 4.080
Atmospheric Temperature	24	4.433 - 4.498
	25	4.482 - 4.549
Cirrus Clouds Water Vapor	26	1.360 - 1.390
	27	6.535 - 6.895
	28	7.175 - 7.475
Cloud Properties	29	8.400 - 8.700
Ozone	30	9.580 - 9.880
Surface/Cloud Temperature	31	10.780 - 11.280
	32	11.770 - 12.270
Cloud Top Altitude	33	13.185 - 13.485
	34	13.485 - 13.785
	35	13.785 - 14.085

Broadly speaking, MODIS applications were gathered into Land, Ocean and Atmosphere. From Table 1 it is clear that Land Application requirements for spatial resolution are more rigorous than those for Ocean Applications. This fact prevents the use of Ocean Products for studying inland water. Moreover, inadequate sensor calibration, problematic atmospheric correction and bio-optical inversion procedures (Hu et al., 2004) also limits their application.

On the other hand, recent work shows that MODIS Land bands have sufficient sensitivity to be useful in various aquatic applications and have been successfully applied for water studies (Li et al, 2003).

TABLE 2 – BANDS AND APPLICATIONS OF MOD 09 (LAND) AND MOD 18 (OCEAN) PRODUCTS

MOD 09	Band width (nm)	MOD 18	Band width (nm)	Application
1	620-670 (50)			Sediments
		13	672-672 (10)	Sediments
		14	673-683 (10)	Phytoplanckton Fluorescence
		15	743-753 (10)	Phytoplanckton Fluorescence
		16	862-877 (15)	Aerosol properties
2	841-876 (35)			
		8	405-420 (15)	Dissolved organic matter
		9	438-448 (10)	Chlorophyll
3	459-479 (20)			Dissolved organic matter
		10	483-493 (10)	Chlorophyll
		11	526-536 (10)	Chlorophyll
4	545-565 (20)	12	546-556 (10)	Phytoplankton scattering

* bands 5 to 7 are not particularly useful for water optical property assessment

The information content in lower spatial resolution data is determined not only by the pixel size but by the ability of distinguishing between subtle signal intensities. The improved radiometric resolution provided by the 12 bit MODIS image may compensate for the losses in spatial resolution compared to the finer yielded by ETM^{+}-like sensors.

The information content, however, is not only a function of the sensor properties but it is also dependent on the landscape variability. The relationship between sensor spatial resolution and the size distribution of ground objects is crucial for assessing its utility. Lake size in the Amazon floodplain, for instance, can span from less than 0.1 km^2 to more than 3000 km^2 (Melack, 1984). Lake shape also affects the information content for a given spatial resolution. At Amazon floodplain lake shape varies enormously from channel lakes encroached between levees and sandbars to round lakes, oxbow lakes, crescent lakes (Melack, 1984).

If a coarse**r** spatial resolution can be compensated by an improved radiometric and spectral resolution as available in MODIS image data, then it may provide a vital tool for studying water movement from river channel to floodplain lakes of the major drainage basin of the world such as Ganges/Brahmaputra, Huangho (Yellow), Amazon, Yangtze, Irrawaddy, Magdalena, Orinoco, Hungho (Red), Mekong, Indus, Mackenzie, Godavari, La Plata, Haiho, Purari, Niger and Mekong.

2. THE STUDY AREA AND DATA SET

Curuai lake floodplain region (Figure 1) was selected due to the presence of lakes of various sizes (from 300 km^2 to less than 0.1 km^2), shapes and water types which spans a wide range of landscape variability.

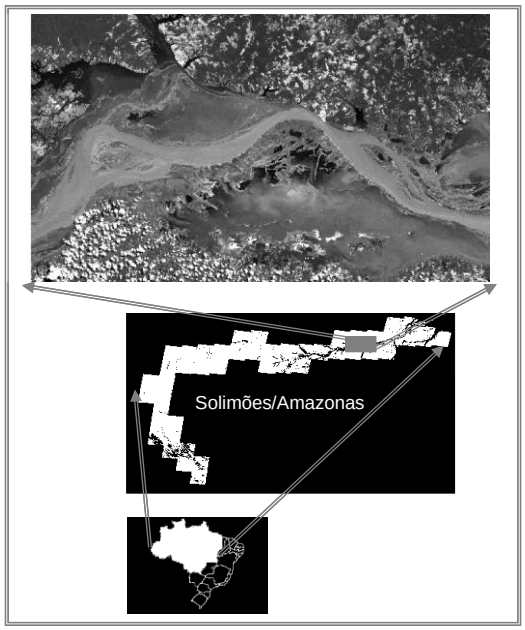

Fig.1 – Curuai lake floodplain test site.

The test site area is located between the towns of Óbidos and Santarém (Pará State), 900 km from the Amazon River mouth and is subject to seasonal fluctuations in water level of around 5.4 m.

The following data set were available for this study: Landsat/ETM $^+$ image (path 228/row 61) and MOD 09 Level 2 G Validated, Version 3 (tile h12v09), both acquired in July 8, 2002. Landsat/ETM $^+$ images were provided by the Image Generation Division at the National Institute for Space Research (INPE) in Geotiff format. MOD 09 product was distributed by the Land Processes Distributed Active Archive Center (LP DAAC), located at the U.S. Geological Survey's EROS Data Center (http://LPDAAC.usgs.gov).

MOD 09 products are available in two sets for Version 3: MODIS GQK set is the MODIS/Terra Surface Reflectance Daily (L2G) Global, 250m resolution, and projected according to an integerized sinusoidal (ISIN) grid. MODIS 250 m Surface Reflectance is a two-band product computed from the MODIS Level 1B land bands 1 and 2 (centered at 648 nm and 858 nm, respectively). MOD09GHK set is the MODIS/Terra Surface Reflectance (L2G) Global, 500 m resolution. It is a seven-band product computed from the MODIS Level 1B land bands 1-7.

Both sets are estimates of the surface spectral reflectance for each band as it would have been measured at ground level if there were no atmospheric scattering or absorption. The correction scheme includes corrections for the effect of atmospheric gases, aerosols, and thin cirrus clouds (http://lpdaac2.usgs.gov/modis/mod09ghk.asp). Table 3 summarizes the main features of each set of MOD 09 product.

TABLE 3 – MOD 09 DATA SE CHARACTERISTICS

MOD09 GQK Data Set Characteristics
Area = ~ 10° x 10° lat/long Image Dimensions = 4800 x 4800 rows/columns Resolution = ~250 meters Projection = Integerized Sinusoidal Data Format = HDF-EOS 16-bit signed int
MOD09GHK Data Set Characteristics
Area = ~ 10° x 10° lat/long Image Dimensions = 2400 x 2400 rows/columns Resolution = ~500 meters Projection = Integerized Sinusoidal Data Format = HDF-EOS 16-bit signed int

3. DATA PROCESSING

The first step in this study consisted in establishing a data base composed of 250 m x 250 m spatial resolution bands. In this step MOD 09 was transformed from the ISIN projection to Lat/Long projection.

This transformation was accomplished by using the MODIS Reprojection Tool (RTM) made available at (http://lpdaac2.usgs.gov/landdaac/tools/modis/about.asp). RTM enables to read data files in HDF-EOS format, select the geographic subset and science data sets as input to processing and performing the geographic transformation to a different coordinate system/cartographic projection. The software also allows defining the pixel size of the output image and writes it in formats other than HDF-EOS.

Bands 3 to 7 of MOD09GHK data set were resample for 250 m using a nearest neighbor algorithm. The output image was saved in Geotiff format. The MOD09 GQK set was only reprojected to Lat/Long and

exported as Geotiff. The final data comprised the seven bands, with a 250 m x 250 m pixel size.

MODIS data is provided as 16 bit data in spite of its inherent 12 bit radiometric resolution. In order to reduce image size, a 16 bit to 8 bit compression was carried out using a tool (Arai et al. 2005) which accommodates the reflectance distribution from the 16 bit image into an 8 bit image by tuning the look up table to users defined reflectance range.

MODIS and ETM$^+$ Image analyses were carried out using SPRING (**Sistema de Processamento de Informações Georeferenciadas**), a freeware Geographical Information and Image Processing System which provides for the integration of raster and vector data format in a single environment (http://www.dpi.inpe.br/spring). MODIS images were registred to ETM$^+$ data and further resampled to 100 m x 100 m (Schowengerdt, 1997).

In order to compare the ability of MODIS images to retrieve land/water boundary with that of ETM$^+$ resampled images, two approaches were tested. The first approach was based on a single band thresholding. The 250 nominal resolution MOD09 B2 (841 – 876 nm) resampled to 100 m x 100m image was selected to build a water surface mask. A mask is a binary image that consists of values of 0 and 1.

This band was selected because of its inherent higher spatial resolution. In the ETM$^+$ data set, infrared band 5 (1.550- 1.750nm) was selected instated of band 4 (0.775- 0.900nm). Preliminary tests showed that the wider sensitivity of band ETM$^+$4 towards the red edge increased its sensitivity to water turbidity resulting in an overlaping of highly turbid water and bare soil.

The second approach to build a water mask was the application of the **linear** unmixing model to MOD 09 and ETM$^+$ data sets (Shimabukuro et al. 1998) so as to determine the relative abundances of shade/water, soil and vegetation cover within a given pixel based on their spectral features. The reflectance at each pixel of the image is assumed to be a linear combination of the reflectance of each material (or endmember) present within the pixel. So given the resulting spectrum (the input data) and the endmember spectra, the linear unmixing solves for the abundance values of each endmember for every pixel. Figure 2 shows the selected endmembers used to run the unmixing algorithm.

In the linear unmixing model, the pixel reflectance (R) at any of the **n** bands can be modeled as the linear combination of the spectral response of **k** pure endmembers. The model can be expressed by (the) a set of linear equations:

$R_i = \Sigma\ (a_{ij}\ x_j\ ) + e_i$, (1)

j=1

where

j = 1, ..., k (endmembers)

i = 1,..., n (bands)

Ri : Pixel reflectance in the ith spectral band.

aij spectral reflectance of the jth endmember at the ith spectral band.

xj : estimated fraction of the jth endmember within the pixel.

The following constraints apply:

$$\sum_{j=1}^{k} x_i = 1 \quad (2)$$

and

0 <= xj <= 1 (3)

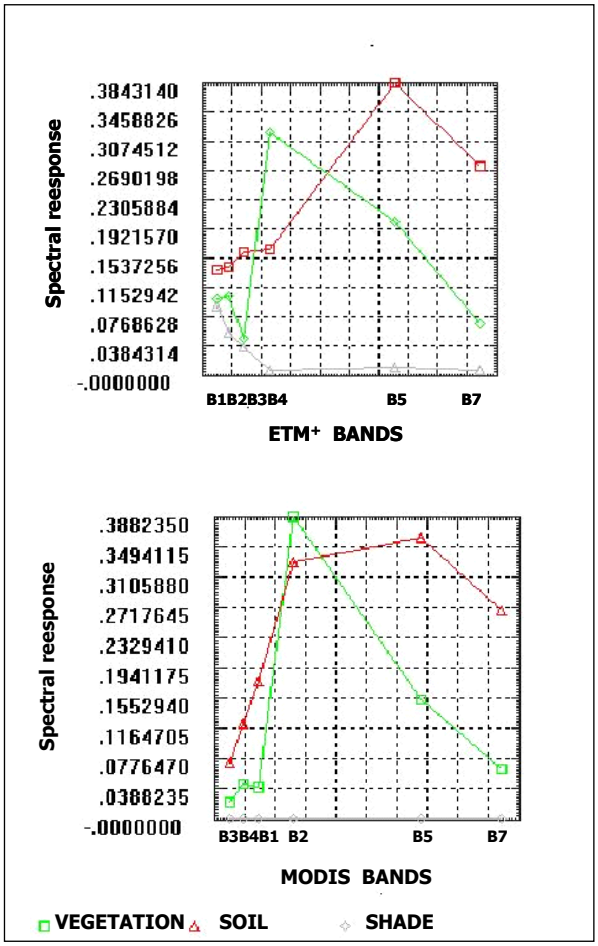

Fig. 2 - Endmember spectral responses (shade, vegetation and soil).

Usually k<n, which makes the system (1) overdetermined. A constrained least squares adjustment approach can be applied here.

The shade fraction was then submitted to image segmentation. In this process individual image pixels are grouped into partitions, according to some intrinsic properties of the image, e.g., gray levels, contrast, spectral values or textural properties (Le

Moigne and Tilton, 1995). In the segmentation a series of *similarity* and *minimum area* thresholds were tested and evaluated against the image color composites in order to select the results fitting both lake and island distribution in the scene. The *similarity* threshold sets the minimum diference between a given pixel digital number and the average digital number in its neighbourhood so as it can be addressed to that region or image segment. The *minimum area* threshold defines the minimum number of pixels to make up a segment. Similarity and minimum area thresholds were set constant in both images.

The rationale for segmenting the fraction image is that if spatial resolution does not affect the discrimination of lakes and island, the number, shape and size of the segments generated in both data sets would be identical. In order to limit the study to the floodplain lakes, a mask was applied to the segmented image to eliminate the Terra Firme rivers and lakes from the analysis. This mask was produced by Hess et al (2004) based on dual date SAR images acquired by JERS1 satellite. The segmented image was then submitted to an unsupervised classification using the Isoseg algorithm available at the SPRING image processing system. It is a region classifier which allows the clustering of segments based on the Mahalanobis distance. The Isoseg is a region classifier. The regions are characterized by the average, covariance matrix and area. The regions are clustered according to a similarity measurement (Mahalanobis distance) between the classes and the candidate regions. The algorithm runs according to three steps: in the first step the user defines an acceptance threshold which will define the distance beyond which the region can not be included in a given cluster. In the second step the algorithm organizes the segments according to their size. The larger segments are assumed to be classes (clusters) for which the statistical parameters are computed. Smaller segments (regions) are then assigned to each cluster according to an acceptance threshold. In the third step the algorithm assigns the segments (regions) to new clusters. The process is repeated up to moment that the clusters statistics did not change from one algorithm run to another The clusters were then assigned manually to. two classes: lakes and islands/land (Schowengerdt, 1997)..

Polygon statistics were produced and analysed in order to quantify the effects of MODIS spatial resolution on the detection of lakes and island. In order to investigate the effect of shape variability on the ability to map island and lakes the Polygon Shape Factor (PSF) was adapted from Wetzel (1976). The PSF is a dimensionless number that expresses the irregularity of the shoreline (perimeter) and the polygon shape departure from a perfect circle. A perfectly circular polygon would have PSF = 1. The PSF can be determined as follows:

$$PSF = p / [2 \sqrt{\pi a}] \quad (4)$$

where

PSF= Polygon Shape Factor;

p= polygon perimeter;

a= polygon area.

4. RESULTS

The results are analyzed according to two approaches. In the first approach the focus is to compare the ability of MODIS and ETM+ image data to retrieve area information.

The second approach consists of comparing ETM+ and MODIS images in relation to their ability to retrieve lake and island shapes.

4.1 Water masks

In this section the results of using a single band versus the shade fraction to create the water mask are compared. The shade fraction image data provided a more accurate rendition of the water surface in the scene than the ETM+ band 5 as shown in the water masks displayed on Figure 3. The advantage of the fraction image lies on its ability for separating water from cloud shadow. It is clear that when ETM+ band 5 is used, the water mask includes cloud shadows (red circle on Figure 3). As the unmixing model takes into account the spectral signature of each pure endmenber, the shade fraction does not include cloud shadow providing a water mask free from this undesirable effect. The shade fraction used to unmix the images shows a very low reflectance in bands 4, 5 and 7. The cloud shadow spectra, however shows a consistent increase in reflectance towards longer infrared wavelengths. It must be pointed out that those are experimental results applicable to the scene characteristics.

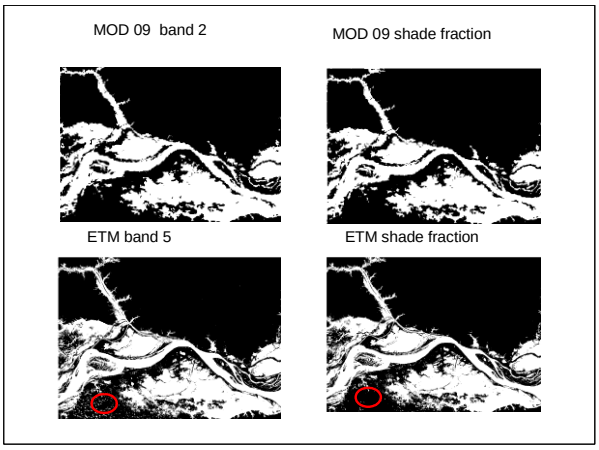

Fig. 3 – The effect of using single bands and the shade fractions on the generation of the Water-Land Mask. Red circle shows the inclusion of cloud shadow in the single ETM$^+$ band 5 mask. This effect is removed when using the ETM$^+$ shade fraction.

As it can be observed in Figure 4 the open water masks derived from the shade fraction did not include the abundant cloud shadow observed in both ETM$^+$ and MOD 09 data set. Total water surface computed from ETM$^+$ and MOD 09 masks are very similar. The total area mapped as water surface is 4731

km^2 and 4205 km^2 respectively, which corresponds to 11 % difference. MOD09 image underestimated the area covered by water because it failed to recover most of the lakes smaller than 0.1 km^2.

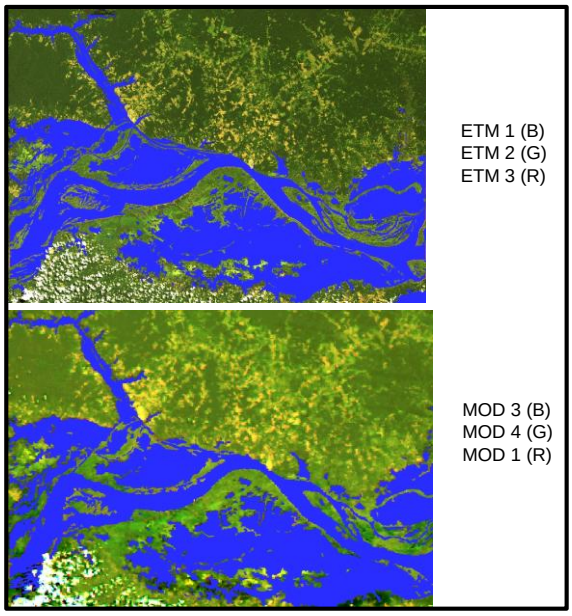

Fig. 4 – Open water shade mask overlaid on ETM+ true color composite and MOD 09 true color composite.

The segmentation of ETM + shade fraction resulted into 2498 polygons whereas the MOD 09 shade fraction resulted in only 1413 polygons. If the polygon size distribution (Figure 5) is analyzed, however, one can observe that there is a close agreement between ETM+ and MOD 09 for class intervals larger than 0.1-1.0 km^2 . Looking into detail within the 0.1 – 1.0 km^2 class intervals it was observed that only in the interval 0.10 to 0.25 km2 there are 486 ETM$^+$ polygons. This class interval corresponds to polygons with area equivalent to 1 to 4 MODIS pixels. Looking into the polygon size distribution for MODIS data it is observed that there are 585 polygons in this size interval. It means that it is not only the size which is responsible for the polygon definition but other variables might explain differences in the detection threshold.

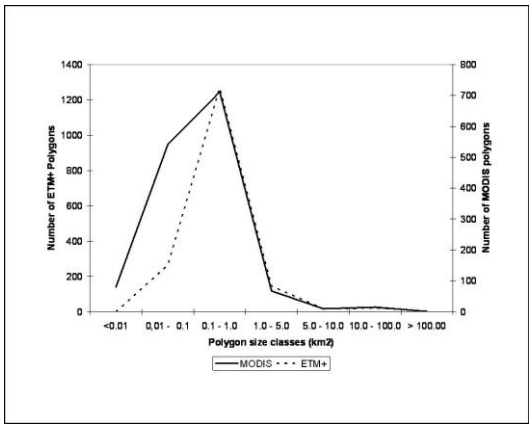

Fig. 5 – ETM$^+$ and MODIS polygon distribution as a function of the area.

4.2 Polygon shape and size distribution

This section explores how the shape of the polygon affects the retrieval of information from both sets of image data.

The more irregular the shape of the polygon, the longer the shoreline will be and the larger the PSF. A rectangular polygon has a Polygon Shape Factor (PSF) around 2, whereas dendritic shaped polygons may have PSF larger than 3. Figure 6 shows the PSF distribution against polygon size for ETM$^+$ (a) and MODIS (b). It is clearly shown that due to the spatial constraints imposed by the MODIS coarse resolution, there is a tighter relationship between PSF and polygon area (Figure 6b). The PSF explains around 68 % (r^2= 0.68) of the detectable lakes and islands when MODIS images are considered whereas for ETM$^+$ images its explanation power drops to 46 % (r^2= 0.46) for the same polygon size interval (Figure 6a).

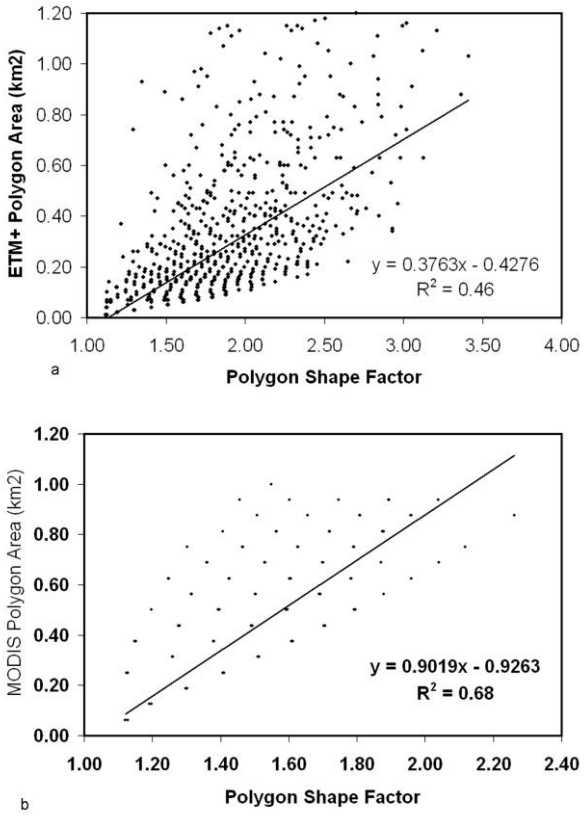

Fig. 6 – Polygon shape factor and polygon area distribution for (a) ETM$^+$ and (b) MODIS image data.

The analysis of figure 6 shows that as the polygon shape departs from a near perfect circle (PSF=1) the polygon size becomes critical. Rectangular polygons (the shape which corresponds to levees, scroll bars and elongated lakes) can only be detected when their surfaces are larger than 0.6 km^2. This restriction is not observed for ETM+ image due to the finer nominal resolution.

Figure 6 also highlights that there are other factors other than the shape affecting sensor ability to detect lakes and islands. Lakes of equal size and shape

can be detected or not as a function of target contrast to the background.

Figure 7 exemplifies this fact. In this figure, island and lake polygons extracted from MODIS (Blue) and from ETM$^+$ images (Red) are overlaid on a MOD 09 true color composite. It is clear in A1 that MOD 09 images missed small long islands with one of the dimensions smaller than 2 pixels. MOD 09 images recovered the general shape and format of the large island in A2 but it was unable to depict the fine detail of channels and small lakes within the island. In B one can observe that it is not only the size and shape that affects the recovering of the ground information. The contrast between the water and its surroundings is also an important variable. In A, the island is within a white water lake where there is a high contrast between the vegetation cover and the water. The island is clearly distinguished against the white background. In B, however, the islands are located in a clear water lake, which represents a dark background against which the island does not produce a detectable signal. In B1 the channel is 1.2 km wide but was not detected due to the low contrast between water and the surrounding vegetation. Another factor affecting the detection is the spatial frequency of the feature. In C1 there is an almost perfect correspondence between ETM+ and MOD 09. In C2, however, the irregular set of levees is not registered by MOD 09 as a continuous surface. D1 and D2 shows that beyond a given size, contrast between lakes and islands are no longer important.

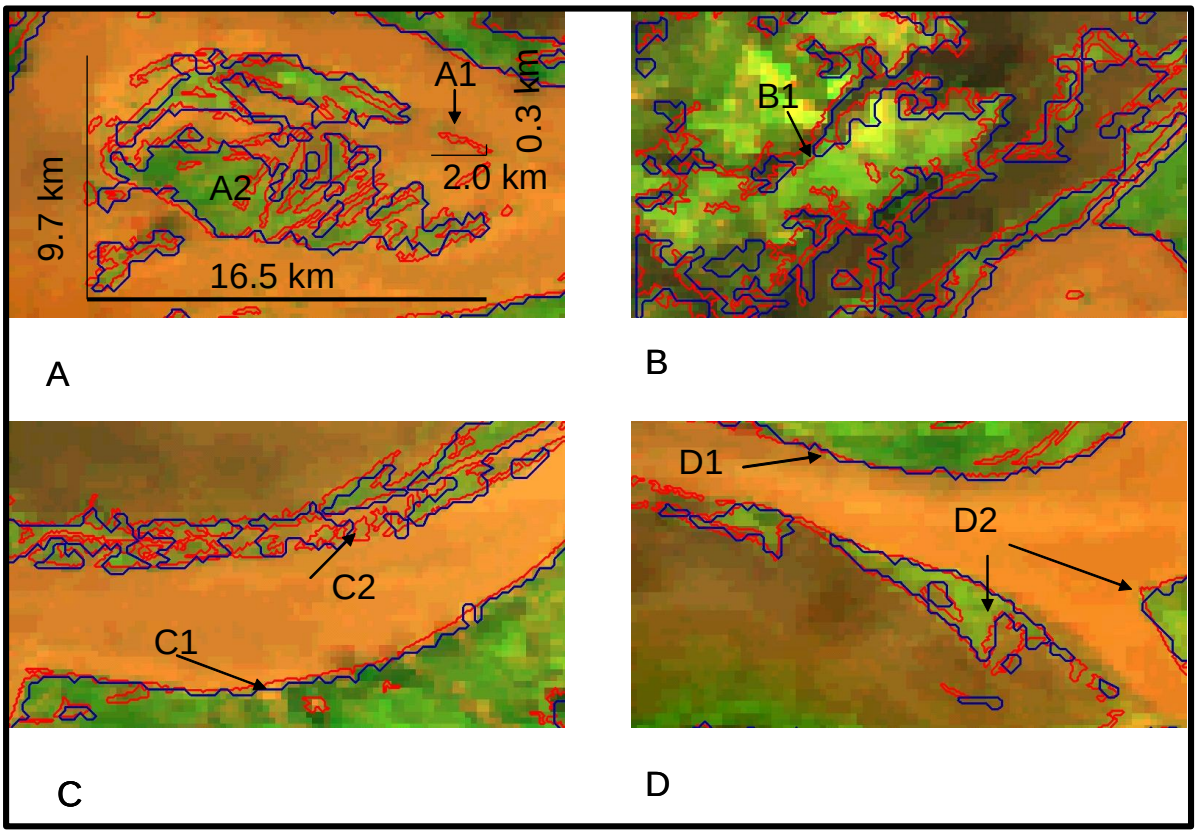

Fig. 7 – Effect of local features on the retrieval of lakes and islands from ETM$^+$ and MOD 09 images.

At a regional scale (Figure 8), the results rendered by the segmentation of both ETM+ and MODIS shade fraction are very similar. The main floodplain features such as river channels, islands, lakes, sand bars, and levees were mapped by both products. The differences are focused on the detection of local features. The finer nominal resolution in ETM image data renders detailed lake shores which are detected by the coarser spatial resolution MODIS data as straight lines. But, in spite of the finer spatial resolution, there features which are not detected by ETM$^+$ and yet are rendered by MODIS. This is observed at the polygon difference images. The cyan polygons identified on ETM$^+$ shade fraction image were missed by the segmentation of MODIS shade fraction image. The statistical analysis showed that most of them (99 %) represent features with sizes smaller than four MODIS pixels. MODIS polygons subtracted from ETM$^+$ polygons overlaid on MODIS true color composite (pink line are polygons which were identified on MODIS shade fraction and not in ETM+ shade fraction) suggests that there are features which can be detected by the MODIS data and overlooked by ETM$^+$ data, suggesting that the improved radiometric and spectral resolution compensates for the coarser spatial resolution. It is important, however, to stress the fact

that in the experiment the ETM$^+$ were degraded to a pixel size of 100m x 100m. The detailed analyses of the polygon difference distribution shows that 74 % of them were in the class size between one and three pixels (0.06 km^2 – 0,125 km^2).

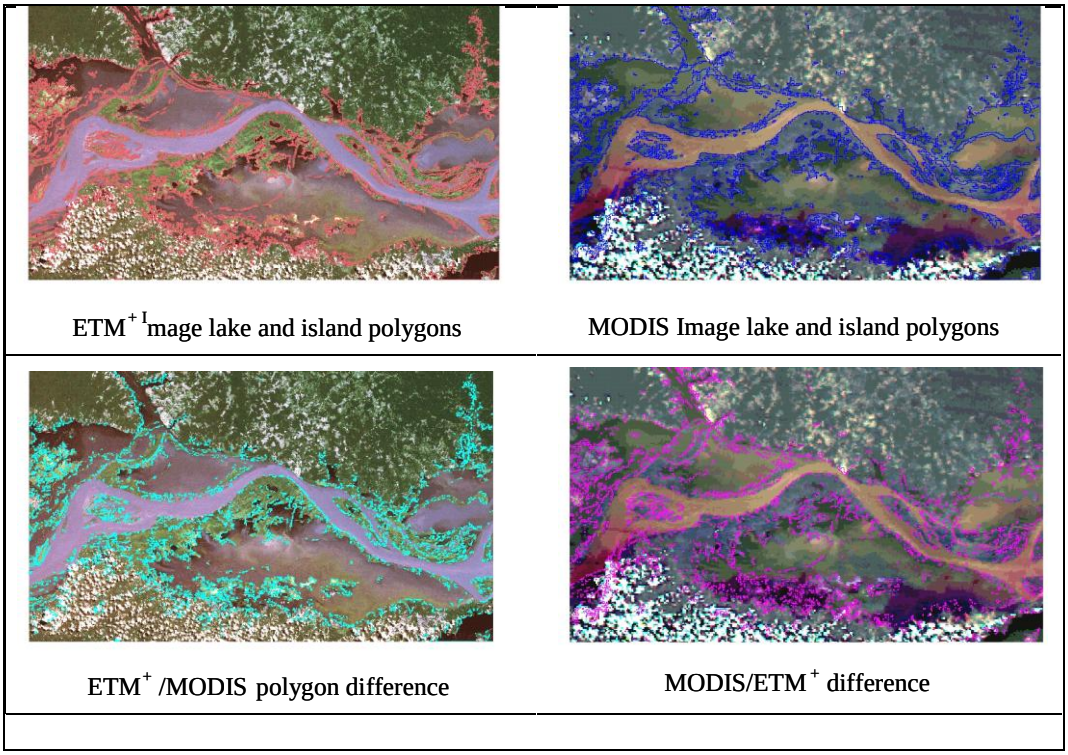

Fig. 8 - Polygons resulting from the segmentation and classification of the – ETM$^+$ and MODIS shade fraction images. The red line corresponds to ETM$^+$ polygons overlaid on ETM$^+$ image data. The blue line corresponds to the MODIS polygons overlaid on MODIS image data. Cyan lines are polygons which were identified only on ETM$^+$ images (ETM$^+$/MODIS polygon difference). Pink lines are polygons which were identified only on MODIS image data (MODIS/ETM difference).

Actually 99 % of the polygons missed by ETM$^+$ segmented shade fraction are smaller then 1 km^2. Those differences can be explained by the increased MODIS radiometric sensitivity which sometimes compensates for the better ETM$^+$ spatial resolution. The analyses of the ETM$^+$- MODIS statistics showed that MODIS shade fraction image failed to identify around 93 % of the polygons with area smaller than four pixels.

5. CONCLUSIONS

The results show that MODIS images underestimated the open water surface in around 11 % in relation to that of ETM$^+$ image. Taking into account that both images were acquired with 05 minutes between takes, those differences are only related to sensor performance in relation to scene features. Although ETM$^+$ was used as reference, it does not mean it renders the correct portrait of the scene. The results presented here show that there are many features identified by MODIS images which were not detected by ETM+ images and the other way around. Batimetric data available for the Curuai lake area will be useful in the future to get a better assessment of the real shape and area of the several lakes and islands. Those studies will help to answer questions such as why in some circumstances the identification limit is 0.25 km^2 (4 MODIS pixels) and in others, the system is able to detect features smaller than 0.125 km^2 (3 MODIS pixels). Features beyond this limit (1 MODIS pixel) were recovered in very special circumstances as shown in this study, but what are those circumstances? Are they constant features in the landscape which would make it easier to forecast MODIS applicability or restrict to very specific cases characterized by a sharp contrast in the intensity of their spectral response and the neighborhood?

The main conclusion at the end of this research is that there are still a lot to be learned about the interactions between sensor specifications and scene response to them.

AKNOWLEDGEMENTS

The authors acknowledge FAPESP for financial support (Grant 2003/00785-3) and Fernanda Titonelli PCI CNPq fellowship which were vital for carrying on this research.

BIBLIOGRAPHICAL REFERENCES

ARAI, E.; FREITAS, R. M.; ANDERSON, L. O. S., Y. E. Análise Radiométrica de Imagens MOD09 em 16bits e 8bits. **Simpósio Brasileiro de Sensoriamento Remoto**, 12 (SBSR) Goiânia, Anais, p:3983-3990, 2005

HESS, L. L.; MELACK, J. M.; NOVO, E.M.L.M.; BARBOSA, C. C. F.; GASTIL, M. Dual-Season Mapping of Wetland Inundation and Vegetation for the Central Amazon Basin. **Remote Sensing of Environment**, 87(4):404-428, 2004.

HU, C.; CHEN, Z. ; CLAYTON, T.D.; SWARZENSKI, P. ; BROCK, J.C. ; MULLER-KARGER, F.E. Assessment of estuarine water-quality indicators using MODIS medium-resolution bands: Initial results from Tampa Bay, Florida**.** ***Remote Sensing of Environment***, Volume 93(3): 423-441, 2004.

JUNK, W. J. **The central Amazon floodplain**: Ecology of a pulsing system. Springer, Ecological Studies 126: 525 pp.,1997.

KAMPEL, M.; NOVO, E.M.L.M. O sensoriamento remoto da cor da água. In**: Oceanografia por satélites**. pp. 179-196. Ed. R.B. Souza, Oficina de Texto, 336 pp., 2005.

KIRK, J.T.O. **Light and photosynthesis in aquatic ecosystems**. New York, 2 Ed., Cambridge Univ. Press, 509 p, 1994.

LE MOIGNE, J.; TILTON, J.C. Refining Image segmentation by integration of edge and region data. **IEEE Transactions on Geoscience and Remote Sensing**, **33** (3): 605-615, 1995.

LI, R. R. ; KAUFMAN, Y.F. ; GAO, B.C. ; DAVIS, C.O. Remote sensing of suspended sediments and shallow coastal waters, **IEEE Transections on Geoscience and Remote Sensing.** 41: 559-566, 2003.

MELACK, J. M. Amazon floodplain lakes: Shape, fetch, and stratification. **Verh. Internat. Verein. Limnol.**, v. 22, p. 1278-1282, 1984.

SCHOWENGERDT, R.A. **Remote sensing: models and methods for image processing**. 2nd edition, Academic Press, New York, 1997. 517 p.

SHIMABUKURO, Y.E.; NOVO, E.M.; PONZONI, F.J. Índice de vegetação e modelo linear de mistura espectral no monitoramento da região do Pantanal. **Pesquisa Agropecuária Brasileira**, 33:1729-1737, 1998.

WETZEL, R. G. **Limnology**. Philadelphia. London. Toronto: W. B. Saunders Company, 1976. 742 p.